International Journal of Environmental Sciences
ISSN: 2229-7359
Vol. 11 No. 6, 2025
https://theaspd.com/index.php

# Comparative Analysis Of Mineral Chemistry Of Two Tsabong Kimberlite Pipes And Charecteristics Of Sub-Continental Mantle Within The Tsabong Kimeberlite Cluster, Kgalagadi District, Botswana.

**Rahul Verma[1], Faith Sebopiwa[1] & H.Lawmkima[2]**
[1]Deptt. Of Geology & Geological Engineering, Botswanan International University of Science and Technology, Palapye, Central District , Botswana, Pincode-00114
[2]Department of Geology, Pachhunga University College, Mizoram University, Aizawl, India, 796001

***Abstract***
*The aim of the project is to conduct a comprehensive comparative analysis of two kimberlites pipes of the Tsabong kimberlite field based on their mineral chemistry and characterise the mantle they sampled. Kimberlites world-wide receive a lot of attention despite their small volumetric significance mainly due to the diamonds they host. Much detailed study, including of emplacement, mantle sources and nomenclature, has been based on the Southern parts of Africa, particularly South Africa, and in Botswana. The main objectives of the project are to study the mineral chemistry (major elements; garnets and clinopyroxenes) of the kimberlite xenocryst to analyse the characteristics that associates them with diamonds in the mantle and to determine the depths from which the kimberlitic suites and mantle xenoliths have been derived. Finally, to establish the temperature and pressure conditions under which xenocrysts were derived from the mantle.*
*The study area is located approximately 35 km southwest of Tsabong village. The area is within Kalahari basin at the western edge of the Kaapvaal craton. The Kalahari region's geology is challenging to study and understand due to the scarcity of outcrops. The geology of Tsabong is predominantly composed of a basement complex consisting of ancient crystalline rocks.*
*Analysis of data and mineral chemistry including the Clinopyroxene Thermobarometry has been performed to meet the objectives. The evaluation of mineral compositions in the Tsabong kimberlite cluster suggests a potentially lower diamond potential. The garnet Cr-Ca plots indicate the predominance of lherzolitic pyrope garnets (G9) at exceptionally low chrome contents. Lherzolitic pyrope garnets signals the entrainment of very fertile mantle at shallow depths for these kimberlites hence the lower diamond potential. For future studies, sample size should be increased by expanding the number of boreholes sampled.*
***Keywords:*** *Tsabong kimberlite, Kaapvaal craton, Clinopyroxene Thermobarometry, Lherzolite*

## INTRODUCTION

### Introduction

Kimberlites represent carbonate- rich volcanic rocks of peridotitic composition of at least 35% olivine derived from the mantle. Kimberlites are deepest sourced low degree melts and the paramount host for diamonds. The geochemistry, mineral chemistry and petrology of these rocks have contributed enormous knowledge to understanding of the evolution of the Earth's interior mainly the continental crust and lithospheric mantle *(Mothobeki, 2019)*.

The subcontinental lithospheric mantle (SCLM) is a part of the Earth's upper mantle that is situated beneath the continental crust. It originated during the Archean period, which spans from approximately 2.5 to 4 billion years ago. According to *Brey, 2018* the SCLM formed through high degrees of partial melting of subducted slabs, followed by metasomatism (chemical alteration) processes.

Various kinds of xenoliths found in the mantle comprise eclogite, peridotite, pyroxenite, and MARIDS (Mica-Amphibole-Rutile-Ilmenite-Diopside). MARIDS are highly metasomatized mantle rocks. They exhibit significant enrichment in alkali metals and volatile components. Additionally, MARIDS xenoliths are known to be rich in carbonate and serpentine minerals. The presence of these minerals suggests extensive chemical alteration and fluid infiltration within the mantle, providing valuable insights into the processes occurring deep within the Earth *(Pearson et al., 2003; Jacob et al., 2009)*.

The study and analyses of the chemical composition of xenocrysts and megacrysts offers valuable insights into the makeup of the lithospheric mantle that is sampled by kimberlites. Xenocrysts, such as garnet and clinopyroxene, harbour a range of trace elements that are both compatible and incompatible with their host rocks. These major elements serve as informative indicators for understanding the chemical characteristics of the lithospheric mantle (*Mothobeki, 2019*).The Tsabong Kimberlite Cluster hosts kimberlites and their associated xenocrysts. However, there is limited or minimal published literature hence several critical geological and geochemical questions remain unanswered i.e., mantle paleogeotherms of Tsabong kimberlites. Moreover, the nature of interactions between kimberlitic melts and the subcontinental lithospheric mantle in this specific geological context remains poorly understood. Therefore, this lacking necessitates a comprehensive investigation.

**Aims and objectives of the project.**

The aim of the project is to conduct a comprehensive comparative analysis of two kimberlites pipes of the Tsabong kimberlite field based on their mineral chemistry and characterise the mantle they sampled.

The main objectives of this research are:

- To study the mineral chemistry (major elements; garnets and clinopyroxenes) of the kimberlite xenocryst to analyse the characteristics that associates them with diamonds in the mantle.
- To determine the depths from which the kimberlitic suites and mantle xenoliths have been derived.
- To establish the temperature and pressure conditions under which xenocrysts were derived from the mantle.

**Location**

The study is located approximately 35 km southwest of Tsabong village, Botswana (Figure 1). The area is within Kalahari basin at the western edge of the Kaapvaal craton. The Kalahari region's geology is challenging to study and understand due to the scarcity of outcrops. The lack of exposed rock formations makes it difficult to directly observe and analyse the underlying geological structures and processes. The two drill boreholes in this study are approximately 9 km apart. The 105_043_0018_H001 borehole is located at longitude E 22° 10' 28.228", latitude S 26° 12' 26.514" and the 105_043_0020_H001 borehole is located at longitude E 22° 7' 37.683", latitude S 26° 15' 58.98".

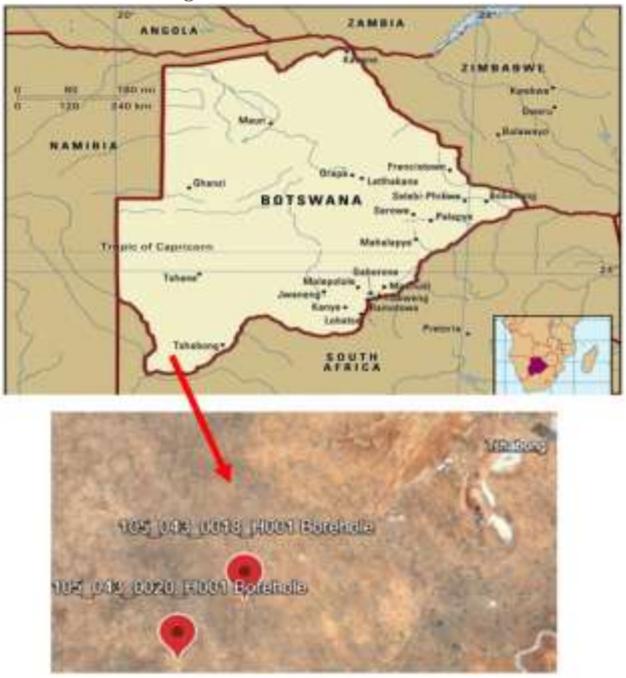


***Fig.1: Location of the Study Area***

## GEOLOGY

### Kaapvaal Craton

The Kaapvaal craton is one of the oldest and well-preserved cratons bounded towards the south with the Namaqua- Natal Proterozoic mobile belt (approximately 1.1–1.9 Ga) and Zimbabwe craton to the North. Both Kaapvaal craton and the Zimbabwe craton are separated by Limpopo mobile belt, a late Archean orogenic belt. The Zimbabwe craton consolidated in late Archean period (3.30-3.55 Ga), and it comprise of a complex named TTG (tonalite, trondhjemite and granodiorite). The kimberlites emplaced through the Kaapvaal craton are believed to have sampled the subcontinental lithospheric mantle as xenoliths. The Kaapvaal craton is known for its low heat flow, which refers to the amount of heat escaping from the Earth's interior through the crust. The craton's low heat flow, around 45 mWm-2 (milliwatts per square meter), contributes to the formation of diamondiferous kimberlites. The cool lithospheric mantle resulting from the low heat flow in the Kaapvaal craton provides favourable conditions for the preservation and concentration of diamonds within kimberlites. Whereas younger orogenic belts generally exhibit higher heat flow, around 80 mWm-2, making it less conducive for the formation of diamond-bearing kimberlites. As a result, orogenic belts with high heat flow are often associated with barren kimberlites that lack economic diamond deposits (*Smildzins,2016*).

### Geology of the Tsabong area

The geology of Tsabong is predominantly composed of a basement complex consisting of ancient crystalline rocks. These rocks originated from the core of the Kalahari craton and are primarily composed of granite, gneiss, and schist. The basement rocks found in Tsabong are overlain by the Karoo supergroup, which consists of sedimentary rocks deposited during the Paleoproterozoic era. These sedimentary formations include quartzites, shales, and dolomites *(Franchi et al., 2021).*

Karoo Supergroup, which represents a significant sedimentary sequence deposited during the late Palaeozoic period. The Karoo Supergroup in the area is represented only by which is the Dwyka Group which is typically characterized by a massive tillite composed of mudstones, siltstones, and sandstones as displayed in (Figure 2). This geological sequence is overlain by a layer of approximately 20 meters of unconsolidated sand that overlays units of calcrete and silcrete. The sand is likely a result of aeolian (wind-driven) processes, which are common in arid regions like the Kalahari. A displacement of these rock units due to faulting or other tectonic activities resulted in a discontinuous pattern of the general strata within the basin resulting in inconsistencies of the stratigraphy.

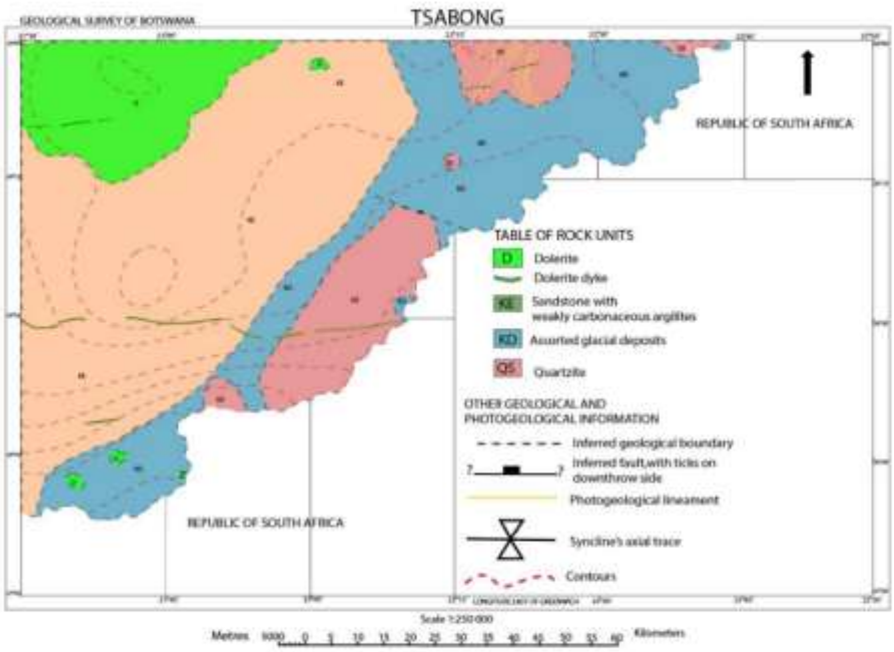


*Figure. 2: Geology of the study are Tsabong (Botswana Geoscience Institute)*

**Tsabong Stratigraphy**

The Tsabong kimberlite pipes themselves penetrate through the Karoo Supergroup, specifically intersecting shales, varved shales, and to a lesser extent, glacial tillites of the Dwyka Group. These Karoo supergroup formations make up the bulk of the material filling these kimberlite pipes, shedding light on the geological history of the region and the unique characteristics of the Tsabong kimberlites. Figure 3 below gives a generalised overview of the stratigraphic sequence of the Tsabong area. The uppermost section, spanning from 0 meters to 105.84 meters, did not yield any core samples, as it is primarily composed of the Kalahari sands, which blanket the underlying rock formations. In the southeastern part of Botswana, the 'Stormberg Lava' group has eroded, revealing the 'Lebung Group,' which was subsequently buried under 70-140 meters of 'Kalahari beds. Beneath the Lebung group is the Beaufort group which intercalate with the Lebung Group . Beaufort Group is underlain by the Ecca and Dwyka Groups.

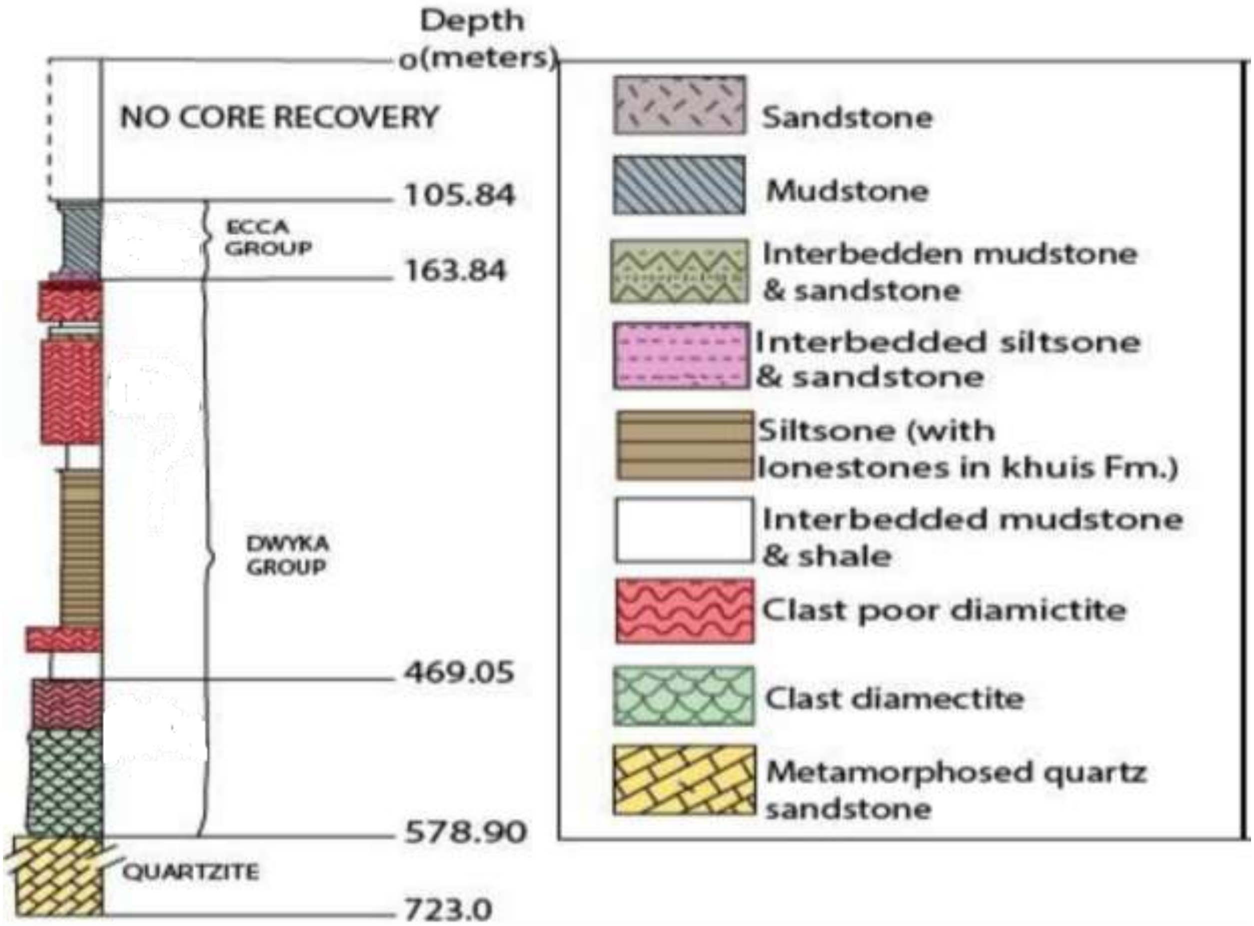


***Figure .3 : Generalized stratigraphic sequence of the Tsabong area (Ndebele, 2020)***

## METHODOLOGY

**Data Sources**

The data source for this research project will be secondary data, specifically mineral chemistry data of major elements provided by De Beers Holdings Botswana (DBHB). The dataset includes information on the mineral composition of samples collected from two Tsabong kimberlite pipes within the Kgalagadi District, Botswana.

**Data Collection and Methods of Investigation**

The mineral chemistry data provided by DBHB was collected from two drill boreholes in Tsabong. The dataset comprises results from extensive testing and analysis conducted by De Beers as part of their exploration operations within the Tsabong kimberlite cluster. The samples for recovery of xenocrysts were selected from the kimberlite drill cores every 20 m throughout the entire length of core for the two boreholes and the composition of major elements (Na, Mg, Al, Si, Ca, Ti, Cr, Mn, Fe and Zn) were extracted and analysed on all recovered xenocrysts (garnet and clinopyroxene) using Electron Probe Micro Analysis (EPMA). The major elements analyses were carried out utilizing the SX-Five EPMA at De Beers Indicator Mineral Laboratory's Analytical Facility.

**Methods of Data Analysis**:

The mineral chemistry data will be subjected to rigorous data analysis, including mineral chemistry analysis using garnets and spinels plots and single clinopyroxene thermobarometry method of *Nimis and Taylor (2000)* will be used to establish the temperature and pressure at the time of xenocryst emplacement. Geotherm software will be used to construct meaningful graphs that will be used to analyze the data. The goal is to compare the mineral chemistry of the two Tsabong kimberlite pipes and, through this analysis, characterize the sub-continental mantle they sampled.

**Mineral Chemistry Analysis**

The chemical compositions of these kimberlites indicator minerals offer substantial information about the genesis of kimberlites. This information includes details such as the depth at which the kimberlite was sampled and data related to the mantle suite, which aids in determining whether the kimberlite is diamond-bearing or not. Furthermore, these methods enable the differentiation of kimberlites and provide a comprehensive evaluation to establish whether they originate from the same source, were formed around the same period, and, most crucially, which one exhibits a greater potential for containing diamonds based on mineral chemistry *(Cookenboo et al., 2010).*

## RESULTS AND DISCUSSION

### CLINOPYROXENE THERMOBAROMETRY

- The Major element compositions (wt.%) of clinopyroxene xenocrysts were used to compute the temperatures and pressures from which they were derived from the mantle. The clinopyroxene major element data was filtered to exclude clinopyroxenes with major element compositions that give errors. The following filters were used:
- Checking the quality of EPMA analyses results i.e., total cations in the range of 3.98-4.02 were used.
- Verification of equilibrium with garnet, clinopyroxenes with $Cr_2O_3$ < 0.5 wt.% and $Al_2O_3$> 4wt.% were excluded.
- Cr values below the range of 0.06-0.50 were used.
- Verification of equilibrium with orthopyroxene, clinopyroxenes with Ca/(Ca+Mg) mol < 0.5wt.% were discarded.
- Iterative calculations produced the following P-T, Tables 1 and 2.

Table 1 shows that Molopo M1 clinopyroxenes were derived from the mantle at an average pressure and temperature of 41kbar and 947 °C. These conditions correspond to depths of approximately 120-140 kilometers beneath the Earth's surface, within the upper mantle.

***Table 1: Major element compositions(wt.%) of the Molopo_M1 kimberlite clinopyroxenes and computed pressures and temperatures.***

| $SiO_2$ | $TiO_2$ | $Al_2O_3$ | $Cr_2O_3$ | FeO | MnO | NiO | MgO | CaO | $Na_2O$ | $K_2O$ | Tot | P (kbar) NG85 | T (°C) TA98 |
|---|---|---|---|---|---|---|---|---|---|---|---|---|---|
| 54.53 | 0.22 | 3.18 | 1.78 | 2.41 | 0.03 | 0.00 | 15.78 | 18.85 | 2.52 | 0.00 | 99.30 | 36.7 | 928 |
| 54.23 | 0.24 | 3.83 | 3.27 | 2.47 | 0.00 | 0.00 | 14.37 | 17.30 | 3.58 | 0.00 | 99.29 | 33.4 | 833 |
| 54.63 | 0.26 | 3.07 | 1.06 | 1.72 | 0.02 | 0.00 | 16.64 | 21.42 | 1.62 | 0.00 | 100.44 | 26.7 | 829 |
| 54.76 | 0.15 | 2.23 | 3.02 | 2.31 | 0.07 | 0.00 | 16.08 | 18.89 | 2.55 | 0.00 | 100.06 | 42.1 | 941 |

| | | | | | | | | | | | | | |
|---|---|---|---|---|---|---|---|---|---|---|---|---|---|
| 54.46 | 0.03 | 1.70 | 2.19 | 2.28 | 0.02 | 0.00 | 16.60 | 20.31 | 1.91 | 0.00 | 99.50 | 43.5 | 901 |
| 54.69 | 0.16 | 3.14 | 2.52 | 2.26 | 0.10 | 0.00 | 15.51 | 18.55 | 2.87 | 0.00 | 99.80 | 37.0 | 888 |
| 54.14 | 0.28 | 2.64 | 1.83 | 2.11 | 0.05 | 0.00 | 16.25 | 19.83 | 2.20 | 0.00 | 99.33 | 36.3 | 870 |
| 54.21 | 0.18 | 2.72 | 2.36 | 2.43 | 0.00 | 0.00 | 15.68 | 19.07 | 2.61 | 0.00 | 99.26 | 38.1 | 860 |
| 54.47 | 0.05 | 1.84 | 1.18 | 2.89 | 0.04 | 0.00 | 19.10 | 18.43 | 1.25 | 0.00 | 99.25 | 49.2 | 1236 |
| 54.28 | 0.16 | 2.54 | 2.86 | 3.04 | 0.13 | 0.00 | 15.44 | 18.67 | 2.57 | 0.00 | 99.69 | 39.4 | 931 |
| 54.82 | 0.07 | 1.30 | 2.02 | 1.82 | 0.07 | 0.00 | 17.38 | 21.18 | 1.24 | 0.00 | 99.90 | 42.5 | 988 |
| 54.39 | 0.59 | 2.39 | 1.38 | 2.91 | 0.08 | 0.00 | 18.28 | 17.15 | 2.04 | 0.00 | 99.21 | 53.0 | 1198 |
| 54.76 | 0.40 | 1.94 | 1.27 | 2.86 | 0.05 | 0.00 | 18.91 | 18.04 | 1.57 | 0.00 | 99.80 | 52.5 | 1220 |
| 54.48 | 0.10 | 1.95 | 1.71 | 2.69 | 0.12 | 0.00 | 18.27 | 18.39 | 1.63 | 0.00 | 99.34 | 48.5 | 1181 |
| 54.58 | 0.21 | 2.46 | 1.25 | 2.38 | 0.09 | 0.00 | 16.91 | 19.70 | 1.98 | 0.00 | 99.56 | 42.3 | 976 |
| 54.22 | 0.37 | 2.26 | 1.22 | 2.61 | 0.09 | 0.00 | 17.38 | 19.23 | 1.86 | 0.00 | 99.24 | 46.5 | 1050 |
| 54.59 | 0.11 | 2.94 | 4.35 | 2.13 | 0.07 | 0.00 | 14.49 | 17.25 | 3.57 | 0.00 | 99.50 | 37.5 | 860 |
| 54.79 | 0.08 | 2.04 | 1.55 | 2.13 | 0.01 | 0.00 | 16.65 | 20.66 | 1.80 | 0.00 | 99.71 | 40.4 | 892 |
| 54.89 | 0.10 | 1.82 | 1.25 | 2.71 | 0.07 | 0.00 | 18.87 | 18.50 | 1.27 | 0.00 | 99.48 | 49.4 | 1235 |
| 55.00 | 0.09 | 1.93 | 1.45 | 2.90 | 0.06 | 0.00 | 18.96 | 17.73 | 1.52 | 0.00 | 99.64 | 51.5 | 1254 |
| 54.76 | 0.14 | 1.93 | 1.41 | 2.63 | 0.09 | 0.00 | 18.54 | 18.43 | 1.52 | 0.00 | 99.45 | 49.8 | 1202 |
| 55.06 | 0.10 | 2.68 | 2.15 | 2.14 | 0.06 | 0.00 | 15.81 | 19.30 | 2.41 | 0.00 | 99.71 | 39.0 | 920 |
| 54.72 | 0.06 | 2.00 | 1.58 | 2.07 | 0.06 | 0.00 | 16.50 | 20.53 | 1.71 | 0.00 | 99.23 | 40.5 | 925 |
| 54.33 | 0.29 | 2.67 | 1.95 | 2.53 | 0.06 | 0.00 | 16.07 | 18.71 | 2.39 | 0.00 | 99.00 | 41.8 | 974 |
| 54.14 | 0.25 | 2.90 | 2.88 | 2.23 | 0.06 | 0.00 | 15.34 | 18.47 | 2.67 | 0.00 | 98.94 | 36.5 | 920 |
| 54.74 | 0.12 | 2.59 | 2.74 | 2.16 | 0.10 | 0.00 | 15.94 | 18.53 | 2.64 | 0.00 | 99.56 | 41.3 | 957 |
| 54.64 | 0.12 | 3.52 | 3.30 | 2.08 | 0.10 | 0.00 | 14.85 | 17.56 | 3.36 | 0.00 | 99.53 | 35.4 | 883 |
| 54.67 | 0.23 | 1.30 | 1.97 | 2.77 | 0.08 | 0.00 | 16.49 | 20.01 | 1.86 | 0.00 | 99.38 | 61.5 | 983 |
| 54.57 | 0.00 | 2.51 | 3.09 | 2.16 | 0.04 | 0.00 | 15.84 | 18.58 | 2.63 | 0.00 | 99.42 | 39.7 | 945 |
| 53.97 | 0.13 | 2.64 | 3.45 | 2.05 | 0.10 | 0.00 | 15.21 | 18.20 | 2.81 | 0.00 | 98.56 | 37.6 | 909 |
| 54.62 | 0.28 | 2.26 | 2.24 | 2.52 | 0.09 | 0.00 | 16.42 | 19.46 | 2.29 | 0.00 | 100.18 | 42.6 | 932 |
| **AVERAGE** | | | | | | | | | | | | **40.9** | **947** |

Table 2 shows that Molopo M31 clinopyroxenes were derived from the mantle at an average pressure and temperature of 46kbar and 1139 °C. These conditions correspond to depths of approximately 140-160 kilometers beneath the Earth's surface, within the upper mantle.

***Table 2: Major element compositions (wt.%) of the Molopo_M31 kimberlite clinopyroxenes and computed pressures and temperatures.***

| $SiO_2$ | $TiO_2$ | $Al_2O_3$ | $Cr_2O_3$ | $FeO_t$ | MnO | NiO | MgO | CaO | $Na_2O$ | $K_2O$ | Tot | P (kbar) NG85 | T (°C) TA98 |
|---|---|---|---|---|---|---|---|---|---|---|---|---|---|
| 54.73 | 0.23 | 2.49 | 1.50 | 3.27 | 0.09 | 0.00 | 19.06 | 16.75 | 1.80 | 0.00 | 99.92 | 48.5 | 1258 |
| 54.38 | 0.22 | 2.47 | 2.10 | 2.39 | 0.09 | 0.00 | 16.45 | 19.36 | 2.21 | 0.00 | 99.67 | 40.1 | 952 |
| 54.27 | 0.21 | 3.75 | 2.14 | 2.49 | 0.08 | 0.00 | 15.87 | 18.59 | 2.52 | 0.00 | 99.92 | 32.4 | 964 |
| 54.52 | 0.21 | 1.65 | 1.87 | 2.87 | 0.11 | 0.00 | 17.44 | 18.08 | 1.79 | 0.00 | 98.54 | 55.4 | 1176 |
| 54.38 | 0.34 | 2.66 | 0.91 | 4.06 | 0.11 | 0.00 | 20.91 | 14.09 | 1.60 | 0.00 | 99.06 | 51.0 | 1367 |
| 55.13 | 0.43 | 3.13 | 1.11 | 4.90 | 0.14 | 0.00 | 20.66 | 12.56 | 1.98 | 0.00 | 100.04 | 50.3 | 1369 |
| 54.72 | 0.25 | 2.19 | 1.99 | 2.41 | 0.06 | 0.00 | 16.57 | 19.34 | 2.11 | 0.00 | 99.64 | 44.3 | 991 |
| 54.52 | 0.13 | 2.22 | 2.60 | 1.97 | 0.06 | 0.00 | 16.15 | 19.55 | 2.18 | 0.00 | 99.38 | 39.3 | 931 |

| | | | | | | | | | | | | | |
|---|---|---|---|---|---|---|---|---|---|---|---|---|---|
| 55.65 | 0.12 | 2.85 | 1.54 | 3.73 | 0.13 | 0.00 | 21.04 | 13.12 | 1.74 | 0.00 | 99.92 | 49.3 | 1402 |
| 54.53 | 0.13 | 1.66 | 1.03 | 3.13 | 0.11 | 0.00 | 18.24 | 19.12 | 1.39 | 0.00 | 99.34 | 54.1 | 1169 |
| 53.82 | 0.64 | 0.73 | 1.24 | 3.59 | 0.15 | 0.00 | 17.87 | 19.92 | 0.94 | 0.00 | 98.90 | 61.2 | 1155 |
| 54.04 | 0.14 | 3.03 | 0.53 | 3.84 | 0.02 | 0.00 | 17.04 | 19.30 | 1.33 | 0.00 | 99.27 | 33.8 | 1106 |
| 52.82 | 1.07 | 1.29 | 1.18 | 3.94 | 0.09 | 0.00 | 16.41 | 21.32 | 1.11 | 0.00 | 99.23 | 42.4 | 898 |
| 54.65 | 0.32 | 1.92 | 2.62 | 3.07 | 0.11 | 0.00 | 15.55 | 18.91 | 2.45 | 0.00 | 99.60 | 49.4 | 948 |
| 55.42 | 0.16 | 2.70 | 0.63 | 4.51 | 0.11 | 0.00 | 21.99 | 13.42 | 1.44 | 0.00 | 100.38 | 51.4 | 1406 |
| **AVERAGE** | | | | | | | | | | | | **46.9** | **1139** |

The P-T results from table 1 and 2 were filtered and fitted to a mantle geotherm using the FITPLOT method of Mather et al. (2011) to compute the conductive geotherm with respect to the pressure and temperature of the xenocrysts. The FITPLOT method requires input parameters to compute the geotherm of the locality.
A maximum depth of 250 km was used to prevent infinite loops.
The mantle potential temperature was kept at 1315 °C.
The heat production of the lithospheric mantle (0 W/m3 Kalahari geotherm), from *Rudnick et al., (1999).*The estimated thickness of the lithosphere is ~215 km and ~220 km for the Molopo M1 and Molopo M31 kimberlite, respectively (Figure 4 & 5). Intersection between the isentrope and the geotherm gives the estimate of the thickness of the lithosphere. The following fit plots were generated:

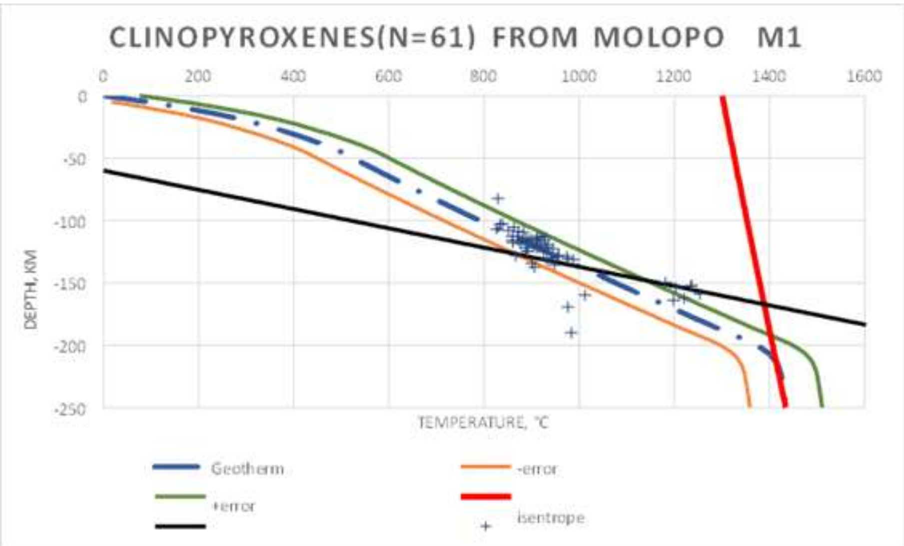


***Figure 4: Plot of Molopo M1 kimberlite P-T data. The P-T data were computed using single clinopyroxene thermobarometry method of Nimis and Grütter (2010).***
The graphite stability field boundary from is Kennedy and Kennedy (1976). The mantle adiabats (1315-1450 °C) are from Pearson et al. (2003). The calculated paleogeotherm lies within the error envelope with few outlies, the outliers indicate poor equilibrium of the samples.
The estimated thickness of the lithosphere is ~215 km for the Molopo M1 kimberlite (Figure 4.1). Most of the xenocrysts fall between 800°C - 1000°C and a depth of 100km to ~145km. Good kimberlites crystallize at these temperatures (850°C -950°C -1000°C). If xenocrysts are derived from these temperatures, it may indicate that they have sampled a good mantle conducive for diamond crystallization. Most of the M1 xenocryst did not sample much of the mantle from the diamond stability field (DSF) or the diamond window, which is greater than 150km (150km - 200km). They were sampled from shallow mantle, which contain para kimberlites. Few xenocrysts plot outside the envelope (+/- error) indicating

that they are not acceptable. These errors relate to the precision of the geothermometer calibration, instrumental drift, and noise during electron microprobe analyses of mineral oxides. These are external errors, unrelated to internal stoichiometry of the minerals.

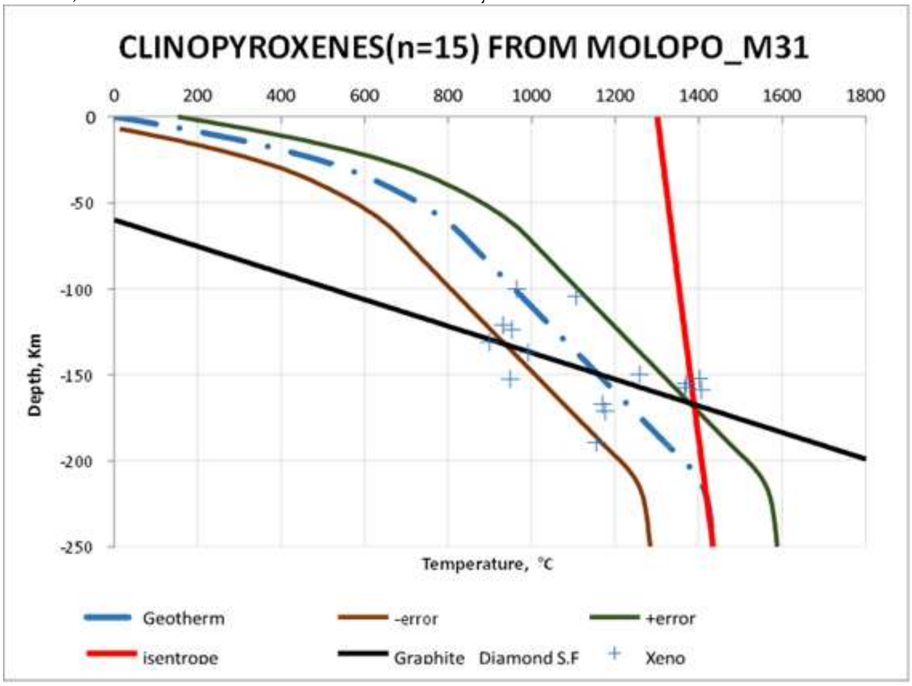


***Figure 5: Plot of Molopo M31 kimberlite P-T data. The P-T data were computed using single clinopyroxene thermobarometry method of Nimis and Grütter (2010).***

The graphite stability field boundary from is Kennedy and Kennedy (1976). The mantle adiabats (1315-1450 °C) are from Pearson et al. (2003). The calculated paleogeotherm lies within the error envelope with few outlies, the outliers indicate poor equilibrium of the samples.

The estimated thickness of the lithosphere is ~220 km for the Molopo M31 kimberlite (Figure 4.2). Most of the xenocrysts within the error envelope in M31 kimberlite fall between 800°C - 1300°C which is the conducive temperature for diamond crystallization. Only 3 xenocrysts within the envelope are derived from the diamond window (150 km to 200 km). They are derived from conducive depths for diamond formation and may carry diamonds. The remaining xenocrysts are derived outside the diamond window with 3 xenocrysts being derived beyond the isentrope or the mantle adiabat possible at the aesthenosphere.

## DISCUSSION

The evaluation of mineral compositions in the Tsabong kimberlite cluster suggests a potentially lower diamond potential. The garnet Cr-Ca plots (Figure 6 & 7) indicates the predominance of lherzolitic pyrope garnets (G 9) at very low chrome contents. Lherzolitic pyrope garnets signals the entrainment of very fertile mantle at shallow depths for these kimberlites hence the lower diamond potential. Both Eclogitic and Harzburgitic garnets are very rare with the latter having very elevated calcium contents plots indicate the presence of pyroxenitic, eclogitic and lherzolitic mantle rocks in the Tsabong kimberlite cluster and no sign of harzburgite. This is shown by low Cr content garnets which indicate shallow, fertile lherzolite which is not expected to contain diamonds. The low chromium content in the garnets implies sampling at shallow depths above the diamond stability zone, reducing the likelihood of encountering diamonds. This trend was consistent across both boreholes analyzed. However, the sample size of the data was so small that it is likely to be less representative of the Tsabong kimberlite field hence susceptible to biasness.

Additionally, chromite plots of Cr-Mg were utilized to characterize the mantle sampled by the boreholes and assess diamond potential. Most grains plotted outside the diamond inclusion window, aligning with the garnet data, indicating sampling of shallow fertile mantle and consequently, a diminished potential for diamonds. It is reasonable to conclude that the M1 and M31 kimberlites likely did not sample mantle from the diamond stability zone.

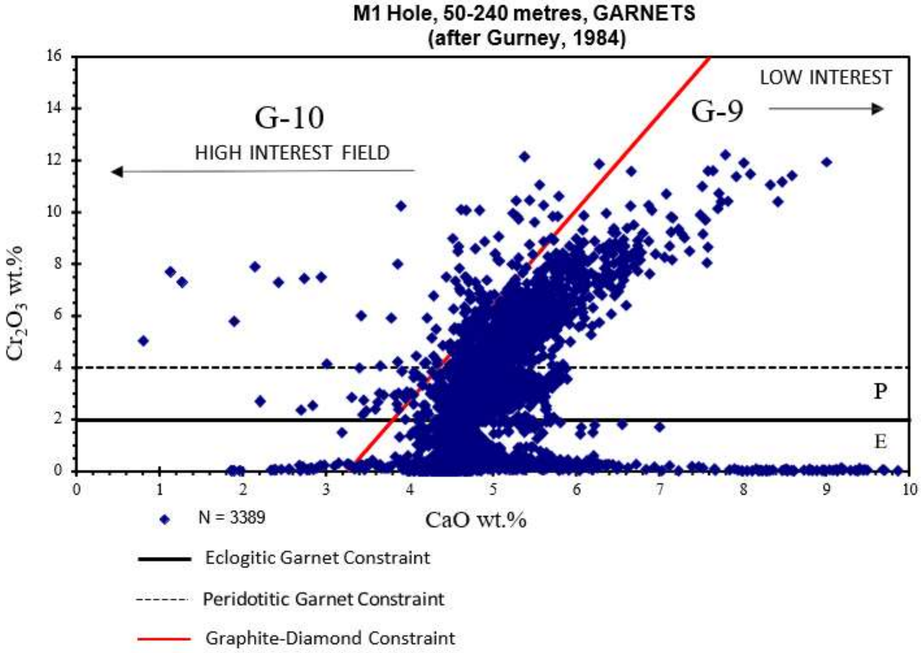


***Figure 6: Cr-Ca diagrams for peridotitic and eclogitic garnet populations from Molopo M31 kimberlite using traditional division***

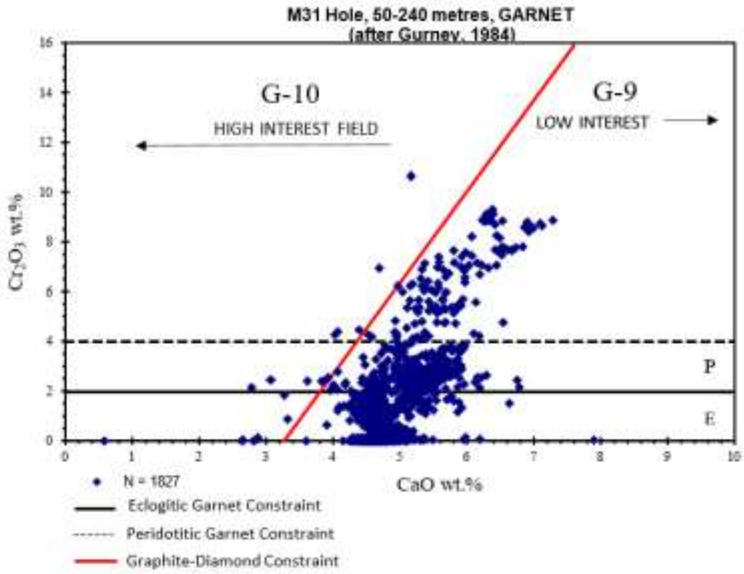


***Figure 7: Cr-Ca diagrams for peridotitic and eclogitic garnet populations from Molopo M31 kimberlite using traditional division.***

Further analysis involved clinopyroxenes to differentiate between various fertile peridotitic and non-peridotitic varieties. Across both boreholes, most of the cpx grains plotted on the on-craton garnet peridotite window (Figures 8 & 9) with only a few grains plotting on the spinel peridotite and off-craton peridotite window and eclogitic field.

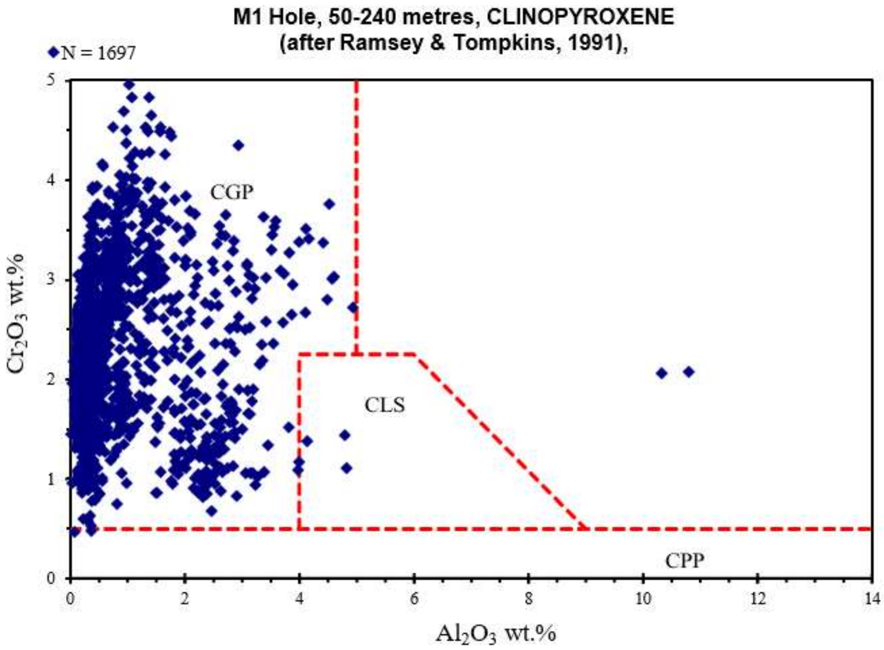


*Figure 8: $Cr_2O_3$ - $Al_2O_3$ plot for Clinopyroxenes populations from Molopo M1 kimberlite.*

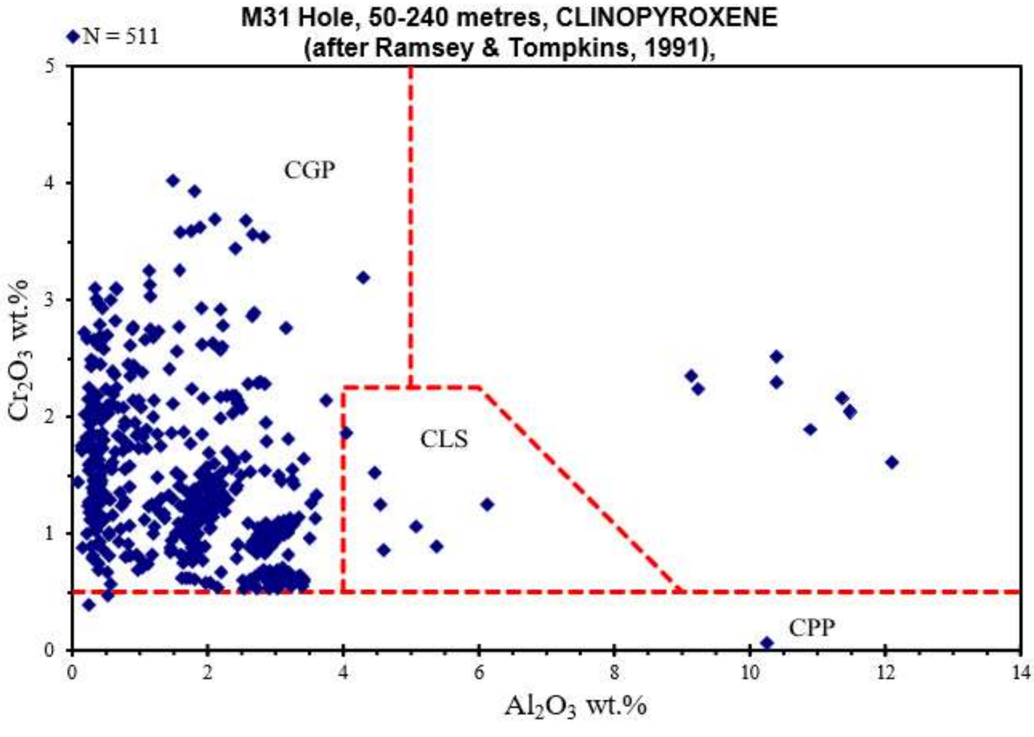


*Figure 9: $Cr_2O_3$ - $Al_2O_3$ plot for Clinopyroxenes populations from Molopo M31 kimberlite.*

## CONCLUSION AND RECOMMENDATION

### CONCLUSION

The results indicate that both kimberlite pipes predominantly sampled shallow, fertile mantle, as evidenced by the presence of lherzolitic pyrope garnets and the absence of harzburgitic garnets. The estimated lithosphere thicknesses and temperature ranges further support this interpretation, suggesting sampling from depths above the diamond stability zone. Additionally, the analysis of clinopyroxenes reinforces the indication of sampling from fertile peridotitic mantle.

## RECOMMENDATION

For future studies, sample size should be increased by expanding the number of boreholes sampled. This would provide a broader dataset, allowing for a more comprehensive and accurate analysis of the geochemistry of the kimberlite. A larger sample size enhances the statistical validity of findings and increases the likelihood of capturing the full range of variability within the studied region.

## ACKNOWLEDGEMENTS

The authors are greatly thankful to De Beers Botswana for providing the research opportunity and granting permission to publish the present work. Authors are also thankful to the Head, Department of Mineral Resources, Botswana International University, and the Department of Geology, P.U.C., Mizoram University, for providing all the necessary permissions to carry out the research.

## COPY RIGHT



### REFERENCES

1. Botswana Geoscience Institute . (2015). Tsabong Sheet 32 Geological map, - 1:125,000
Cookenboo, H.O. and Grütter, H.S. (2010). Mantle-derived indicator mineral compositions as applied to diamond exploration.
2. Franchi, F., Kelepile, T., Di Capua, A., De Wit, M.C., Kemiso, O., Lasarwe, R. and Catuneanu, O. (2021). Lithostratigraphy, sedimentary petrography and geochemistry of the Upper Karoo Supergroup in the Central Kalahari Karoo Sub-Basin, Botswana. *Journal of African Earth Sciences*.
3. Jacob, D.E., Viljoen, K.S. and Grassineau, N.V. (2009). Eclogite xenoliths from Kimberley, South Africa—a case study of manle metasomatism in eclogites. *Lithos*, *112*, pp.1002-1013.
4. Kennedy, C. Scott. & Kennedy, George C. (1976). The equilibrium boundary between graphite and diamond,Journal of Geophysical Research, Volume.81, Issue14. Solid Earth and Planets, pp. 2467-2470
5. Mothobekhi, L. M. (2019). Characteristics of Sub-Continental Lithospheric Mantle Sampled by Group 1 and Group 2 Kimberlites within the Glen Ross Cluster, Barkly West, Northern Cape Province, South Africa.Unpublished Bachelor of Science Honours thesis, University of Witwatersrand.
6. Ndebele, M. (2020). Internal geology and emplacement processes of Kimberlites, Case Study from the Tsabong Kimberlite Field, Botswana. Unpublished master's thesis, Geosciences Department, Luleå University of Technology.
7. Nimis, P & Grutter, H. (2010). Erratum to: Internally consistent geothermometers for garnet peridotites and pyroxenites, Contrib Mineral Petrol. Vol. 159., pp.429–436.
8. Nimis, P. and Taylor, W.R. (2000). Single Clinopyroxene Thermobarometry for Garnet Peridotites. Part I. Calibration and Testing of the Cr-in-Cpx Barometer and an Enstitite-in-Cpx Thermometer. Contributions to Mineralogy and Petrology, Vol., pp. 541-554.
9. Pearson, D.G., Canil, D., and Shirey, S.B. (2003). Mantle samples included in volcanic rocks: xenoliths and diamonds. *Treatise on geochemistry*, *2*, p.568.
10. Rudnick, R. L., Trevor R.I,, Gehrels, G., Hanchar, J.M., Irving, A.J. & Chesley, J.T. (1999). Dating mantle metasomatism: U-Pb geochronology of zircons in cratonic mantle xenoliths from Montana and Tanzania, n book: The P.H. Nixon Volume, Proceedings of the VIIth International Kimberlite Conference, Publisher: Red Roof Design, Editors: J.J. Gurney, J.L. Gurney, M.D. Pascoe, S.H. Richardson, pp.728-736.
11. Smildzins, V. (2016). *Using mineral chemistry to constrain PT conditions for mantle xenoliths from the Kaapvaal craton, South Africa* .master's thesis Oulu Mining School University of Oulu 2016.90p.